Proc. Indian Acad. Sci. (Earth Planet. Sci.), Vol. 98, No. 4, December 1989, pp. 327–338.

Effect of filtering on drift and anisotropy parameters determined by full correlation analysis

H CHANDRA
Physical Research Laboratory, Navrangpura, Ahmedabad 380009, India

MS received 26 July 1989

Abstract. The effect of low-pass filtering on the various drift and anisotropy parameters obtained by full correlation analysis of spaced receiver records is studied theoretically, assuming Gaussian correlation functions. A decrease in the characteristic velocity V_c is shown with increasing filtering, unless $V \gg V_c$, when V_c increases with filtering. The ratio V_c/V however shows an increase as the decrease in the true drift velocity V is steeper than V_c. An increase in the size of the ground pattern with increasing filtering is also shown, while the axial ratio for anisotropic patterns shows a decrease. The results are verified with experimental data recorded earlier at Tiruchirapalli.

Keywords. Filtering; drift; anisotropy parameters; full correlation analysis.

1. Introduction

The effect of filtering-spaced receiver fading records before subjecting them to full correlation analysis was first reported by Sprenger and Schminder (1969). The apparent drift velocity however was found to be independent of filtering. Chandra and Briggs (1978) studied the effect theoretically and showed that the true drift velocity must change with filtering, and argued therefore that this need not be taken as an evidence for dispersion. They also showed that the apparent drift velocity is unchanged by filtering, as the filtering affects only the shape of a correlation function, not the position of its peak (unless there is dispersion when peak position will also shift with filtering). The results were confirmed by applying numerical filters to a number of records obtained using the partial reflection drift experiment at Buckland Park, South Australia.

The effect of low-pass filters on other parameters like the characteristic or the random velocity V_c, the ratio V_c/V, the scale size and the axial ratio of the characteristic ellipse r is studied here on theoretical grounds. The results are then confirmed by applying numerical filters to a few records obtained earlier at an equatorial station, Tiruchirapalli.

2. Theory of correlation analysis

For simplicity we consider the one-dimensional case and a Gaussian form of the correlation functions. Following Briggs *et al* (1950) and Briggs (1968) the temporal auto- and cross-correlation functions are then

$$\rho(0,\tau) = \exp - [(V^2 + V_c^2)\tau^2/\xi_1^2]), \tag{1}$$

$$\rho(\xi_0,\tau) = \exp - \{[(\xi_0 - V\tau)^2 + V_c^2\tau^2]/\xi_1^2\}, \tag{2}$$

where ξ_0 is the receiver separation and ξ_1 is a measure of the scale of the pattern. The spatial correlation function is of the form

$$\rho(\xi,0) = \exp - (\xi^2/\xi_1^2). \tag{3}$$

The maximum value of the cross-correlation function, ρ_m and the time lag τ' at which it occurs can be found from (2) and are given by the following equations

$$\tau' = \xi_0 V/(V^2 + V_c^2), \tag{4}$$

$$\rho_m = \exp - [(V_c^2\xi_0^2)/(V^2 + V_c^2)\xi_1^2]. \tag{5}$$

The apparent drift speed V' is therefore

$$V' = \xi_0/\tau' = (V^2 + V_c^2)/V, \tag{6}$$

To find the true drift speed and other parameters of the characteristic ellipse, a knowledge of the time displacement τ_1 for which the auto-correlation function is equal to the cross-correlation function at zero time lag is required. τ_1 can also be found from the time lag τ_m for which the auto-correlation function is equal to the maximum of the cross-correlation function ρ_m using the relation derived by Fooks (1965)

$$\tau_1^2 = \tau'^2 + \tau_m^2, \tag{7}$$

τ_1 can easily be obtained from equations (1) and (2)

$$\tau_1 = \xi_0/(V^2 + V_c^2)^{1/2}. \tag{8}$$

The fading velocity V_c' is defined by the relation

$$V_c' = \xi_0/\tau_1 = (V^2 + V_c^2)^{1/2}, \tag{9}$$

and V can be found from the well-known relation $V'V = V_c'^2$. An alternative way of finding the true drift V is from the time lag τ_e for which the auto- and cross-correlation functions are equal. This comes out to be

$$\tau_e = \xi_0/2V, \tag{10}$$

and the true drift velocity can be found by this relation. For determining scale sizes one needs in addition the time lag $\tau_{0\cdot 5}$ for half-autocorrelation value. This can be obtained from (1) and (2) and is

$$\tau_{0\cdot 5} = [-\ln(0\cdot 5)]^{1/2}\xi_1/(V^2 + V_c^2)^{1/2}. \tag{11}$$

The scale size ξ_s is defined as the spatial separation for half-correlation, and is calculated by multiplying V_c' with $\tau_{0\cdot 5}$

$$\xi_s = [-\ln(0\cdot 5)]^{1/2}\xi_1. \tag{12}$$

This follows more simply from (3).

3. Effect of filtering on correlation functions

The general effect of filtering on the correlation functions is broadening in case of low-pass filters, and narrowing in case of high-pass filters. The position of the maximum of the cross-correlation function usually remains unaffected (it changes only if there is dispersion when cross-correlation function is asymmetric). Chandra and Briggs (1978) have shown mathematically that use of a low-pass filter will modify the auto- and cross-correlation functions which become

$$\rho(0,\tau) = \exp - [(V^2 + V_c^2)\tau^2/(\xi_1^2 + (V^2 + V_c^2)/\pi^2 f_0^2)], \tag{13}$$

$$\rho(\xi_0,\tau) = \exp - \left[\frac{(\xi_0 - V\tau)^2 + V_c^2\tau^2 + (\xi_0^2 V_c^2/\pi^2 f_0^2 \xi_1^2)}{\xi_1^2 + (V^2 + V_c^2)/\pi^2 f_0^2}\right]. \tag{14}$$

Here the filter function is of the form

$$|Y(f)|^2 = \exp - (f^2/f_0^2), \tag{15}$$

and f_0 is a measure of the cut-off frequency. It was also shown by them that τ_e is modified to

$$(\tau_e)_{f_0} = \xi_0/2V[1 + V_c^2/\pi^2 f_0^2 \xi_1^2]^{-1}, \tag{16}$$

hence the true drift velocity is given by

$$V_{f_0} = V[1 + V_c^2/\pi^2 f_0^2 \xi_1^2]^{-1}. \tag{17}$$

A decrease of the true drift velocity with increasing filtering is noticed from (17) as discussed by Chandra and Briggs.

The various time lags used in the correlation analysis can be found from (13) and (14)

$$\tau'_{f_0} = \xi_0/(V^2 + V_c^2), \tag{18}$$

$$(\rho_m)_{f_0} = \exp - [\xi_0^2 V_c^2/\xi_1^2(V^2 + V_c^2)], \tag{19}$$

$$(\tau_1)_{f_0} = (\xi_0/(V^2 + V_c^2)^{1/2})[1 + V_c^2/\pi^2 f_0^2 \xi_1^2]^{1/2}, \tag{20}$$

and

$$(\tau_{0\cdot 5})_{f_0} = \{[-\ln(0\cdot 5)/(V^2 + V_c^2)][\xi_1^2 + (V^2 + V_c^2)/\pi^2 f_0^2]\}^{1/2}. \tag{21}$$

Thus τ', ρ_m are unaffected by filtering; hence the apparent drift velocity V' remains independent of filtering. The time lag $(\tau_1)_{f_0}$ changes with filtering according to equation (20). Hence

$$(V'_c)_{f_0} = \xi_0/(\tau_1)_{f_0} = (V^2 + V_c^2)^{1/2}[1 + V_c^2/\pi^2 f_0^2 \xi_1^2]^{-1/2}. \tag{22}$$

Substituting $(V'_c) = (V^2 + V_c^2)^{1/2}$ from (8)

$$(V'_c)f_0 = V'_c[1 + (V_c^2/\pi^2 f_0^2 \xi_1^2)]^{-1/2}, \tag{23}$$

therefore V'_c will show a decrease with filtering unless $V_c^2/\pi^2 f_0 \xi_1^2 \ll 1$ or $f_0 \gg V_c/\xi_1$. As f_0 approaches infinity it will approach the correct value, and also as $(V'_c)^2 = V'V$ this implies V_{f_0} will also decrease with filtering in the same manner as $(V'_c)^2_{f_0}$.

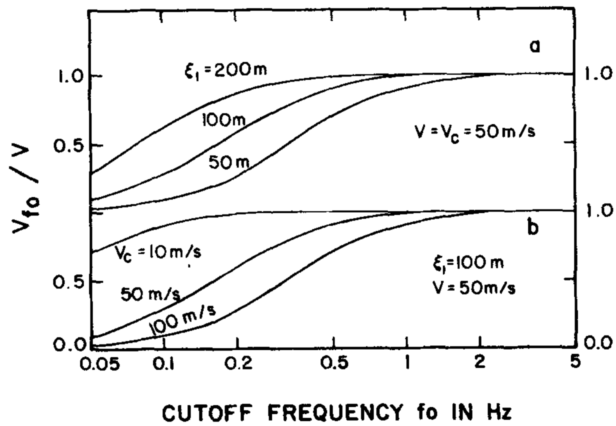

Figure 1. Theoretical variation of the ratio of true drift velocity V_{f_0} obtained using a low pass filter with cut-off frequency f_0 and the true drift velocity V as a function of f_0 for (**a**) three cases with $\xi_1 = 50$, 100, and 200 m respectively and V, V_c constant at 50 m/s, (**b**) three cases with $V_c = 100$, 50 and 10 m/s respectively and ξ_1, V constant at 100 m and 50 m/s.

The effect of low-pass filtering on the true drift was earlier described by Chandra and Briggs (1978). However, for completeness the variation of the ratio V_{f_0}/V as a function of cut-off frequency is shown here in figure 1. The upper half of the figure shows the variation of the ratio V_{f_0}/V for different scale size values of 50, 100 and 200 m with V equal to V_c(50 m/s). The decrease of the ratio is more pronounced the smaller the scale size. For a scale size of 200 m there is no filtering effect at $f_0 > 0{\cdot}5$ Hz. For a scale size value of 100 m the effect is not seen at $f_0 > 1$ Hz, while for 50 m scale size the effect is not seen for $f_0 > 2{\cdot}5$ Hz. The scale size values of 100–200 m and velocities V and V_c of about 50 m/s are typical values for the diffraction patterns associated with ionospheric drifts and partial reflections from the D-region. Since the effect is related to the quantity V_c/ξ_1 computations have also been made for different values of V_c keeping ξ_1, V constant. The variations of the ratio V_{f_0}/V for three different values of V_c equal to 10, 50 and 100 m/s are shown in the lower half of figure 1. Here ξ_1 and V have values of 100 m and 50 m/s respectively. The effect is larger for a large value of V_c. Thus the ratio V_c/ξ_1 determines the change in true drift. In figures 1a and 1b the lower two curves are identical for they represent V_c/ξ_1 equal to 1 and 1/2 respectively.

4. Effect of filtering on the characteristic velocity V_c

To find the effect of filtering on the characteristic velocity V_c, use is made of the well-known relation $V' V = V^2 + V_c^2$. Therefore

$$V_c^2 = V(V' - V), \tag{24}$$

hence

$$(V_c^2)_{f_0} = V_{f_0}(V' - V_{f_0}). \tag{25}$$

The values of $(V_c)_{f_0}$ can be obtained from (25) as V' is independent of filtering, and $(V)_{f_0}$ is already known. To find the effect of filtering on V_c we write the above equation in a slightly different form i.e.

$$(V_c^2)_{f_0} = V_{f_0}[V' - V(1 + V_c^2/\pi^2 f_0^2 \xi_1^2)^{-1}]. \tag{26}$$

Approximate solutions of this equation can be found under different assumptions.

(a) $V_c^2/\pi^2 f_0^2 \xi_1^2 \ll 1$. With this assumption

$$(V_c)_{f_0}/V_c \approx (V_{f_0}/V)^{1/2}. \tag{27}$$

Since for cases $V_c^2/\pi^2 f_0^2 \xi_1^2 \ll 1$, $(V)_{f_0}$ is independent of filtering, $(V_c)_{f_0}/V_c$ will also be unchanged. The ratio $(V_c/V)_{f_0}(V_c/V)$ will also be unchanged.

(b) $V_c^2/\pi^2 f_0^2 \xi_1^2$ much less than 1 but significant. In this case

$$(V_c)_{f_0}/V_c \approx (V_{f_0}/V)^{1/2}[1 + V^2/\pi^2 f_0^2 \xi_1^2]^{1/2}. \tag{28}$$

If in addition $V^2/\pi^2 f_0^2 \xi_1^2 \ll 1$ then

$$(V_c)_{f_0}/V_c \approx (V_{f_0}/V)^{1/2}. \tag{29}$$

This shows that $(V_c)_{f_0}$ will decrease with filtering but the decrease will be less than the decrease in $(V)_{f_0}$. The ratio $(V_c/V)_{f_0}/(V_c/V)$ will increase, however, since

$$(V_c/V)_{f_0}/(V_c/V) \approx (V/V_{f_0})^{1/2}. \tag{30}$$

For conditions $V^2/\pi^2 f_0^2 \xi_1^2 \gg 1$

$$(V_c)_{f_0}/V_c \approx (V_{f_0} V)^{1/2}/\pi f_0 \xi_1 \approx (V/\pi f_0 \xi_1)[1 + V_c^2/\pi^2 f_0^2 \xi_1^2]^{-1/2}. \tag{31}$$

Since under these assumptions most of the changes will come from the term outside the bracket, the ratio $(V_c)_{f_0}/V_c$ will increase due to filtering. The ratio $(V_c/V)_{f_0}/(V_c/V)$ will also increase as given by the relation

$$(V_c/V)_{f_0}/(V_c/V) \approx (V/V_{f_0})^{1/2}(V/\pi f_0 \xi_1). \tag{32}$$

(c) $V_c^2/\pi^2 f_0^2 \xi_1^2 \gg 1$. For this case equation (26) can be simplified to

$$(V_c)_{f_0} \approx (V_{f_0} V')^{1/2}, \tag{33}$$

$$(V_c)_{f_0}/V_c \approx (V_{f_0}/V)^{1/2}, \tag{34}$$

$$\approx [1 + V_c^2/\pi^2 f_0^2 \xi_1^2]^{1/2}. \tag{35}$$

Once again there will be decrease in $(V_c)_{f_0}$. The ratio $(V_c/V)_{f_0}/(V_c/V)$ will increase as given by

$$(V_c/V)_{f_0}/(V_c/V) \approx (V/V_{f_0})^{1/2} \approx [1 + V_c^2/\pi^2 f_0^2 \xi_1^2]^{1/2}. \tag{36}$$

The effect of filtering on V_c is shown in figures 2a, b. The computations are made from the general relation (equation (25)). In figure 2a are shown the variations in $(V_c)_{f_0}/V_c$ with f_0 for scale size values of 50, 100 and 200 m, V, V_c being 50 m/s. The ratio $(V_c)_{f_0}/V_c$ is unaffected for $f_0 > 1$ Hz. At lower f_0 values it decreases, the decrease being more pronounced for smaller scale size. For an f_0 value of 0·05 Hz $(V_c)_{f_0}/V_c$ is about 0·7 for $\xi_1 = 200$ m, 0·42 for $\xi_1 = 100$ m and 0·23 for $\xi_1 = 50$ m. Comparing these

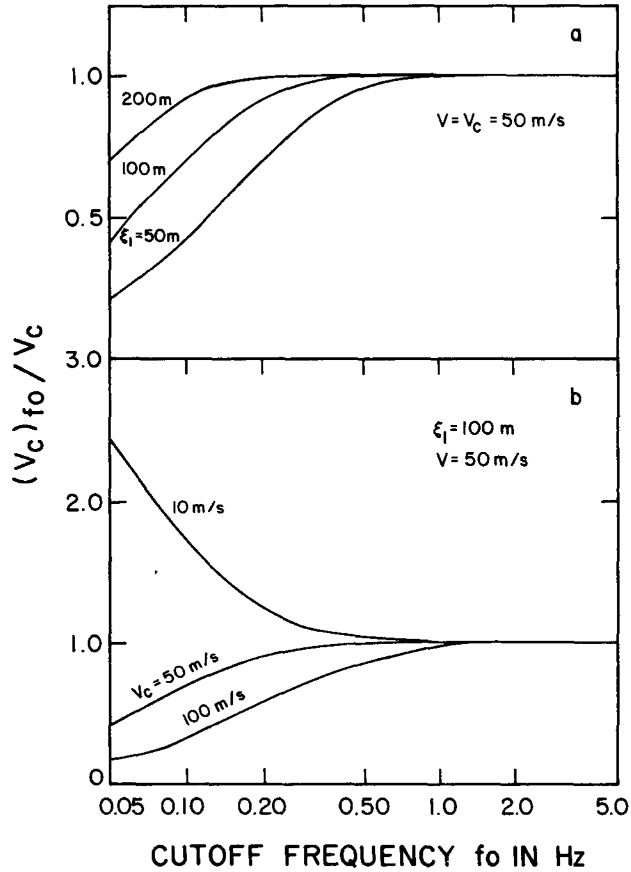

Figure 2. Theoretical variation of the ratio of characteristic velocity $(V_c)_{f_0}$ obtained using a low-pass filter with cut-off frequency f_0 to the characteristic velocity V_c as a function of f_0 for three cases (**a**) $\xi_1 = 50$, 100 and 200 m respectively and V, V_c constant at 50 m/s, (**b**) $V_c = 10$ m/s, 50 m/s and 100 m/s, $V = 50$ m/s and $\xi_1 = 100$ m.

values with $(V_{f_0})/V$ at 0·05 Hz *i.e.* 0·28, 0·09 and 0·02 the decrease in $(V_c)_{f_0}/V_c$ is smaller than in V_{f_0}/V. This is expected as the decrease in V_{f_0}/V is proportional to $[1 + V_c^2/\pi^2 f_0^2 \xi_1^2]^{-1}$ while for $(V_c)_{f_0}/V_c$ it is proportional to $[1 + V_c^2/\pi^2 f_0^2 \xi_1^2]^{-1/2}$.

As the effect of filtering on $(V_c)_{f_0}$ has been shown to be dependent on the relative values of V, V_c and ξ_1 we have computed $(V_c)_{f_0}/V_c$ for different values of V_c and the results of the computations are shown in figure 2b, for $\xi_1 = 100$ m and $V = 50$ m/s. Here the curves for $V_c = 50$ m/s and 100 m/s are similar to those shown in figure 2a. However, for $V_c = 10$ m/s there is an increase rather than a decrease. This is in accordance with (32) which is for conditions $V_c^2/(\pi^2 f_0^2 \xi_1^2) \ll 1$ and $V^2/(\pi^2 f_0^2 \xi_1^2) \gg 1$ or when $V \gg V_c$. The increase in this case can be approximately represented by $V/\pi f_0 \xi_1$. Therefore it will be a function of V/ξ_1. Hence larger V and smaller ξ_1 will result in greater increase in the ratio $(V_c)_{f_0}/V_c$.

The ratio of the characteristic velocity to true drift velocity has similarly been evaluated and the variations of $(V_c/V)_{f_0}/(V_c/V)$ for different scale size and V_c values are shown in figures 3a, b. Figure 3a shows the variations at scale size values of 50, 100 and 200 m with $V = V_c = 50$ m/s. The ratio remains unaffected beyond 2 Hz but

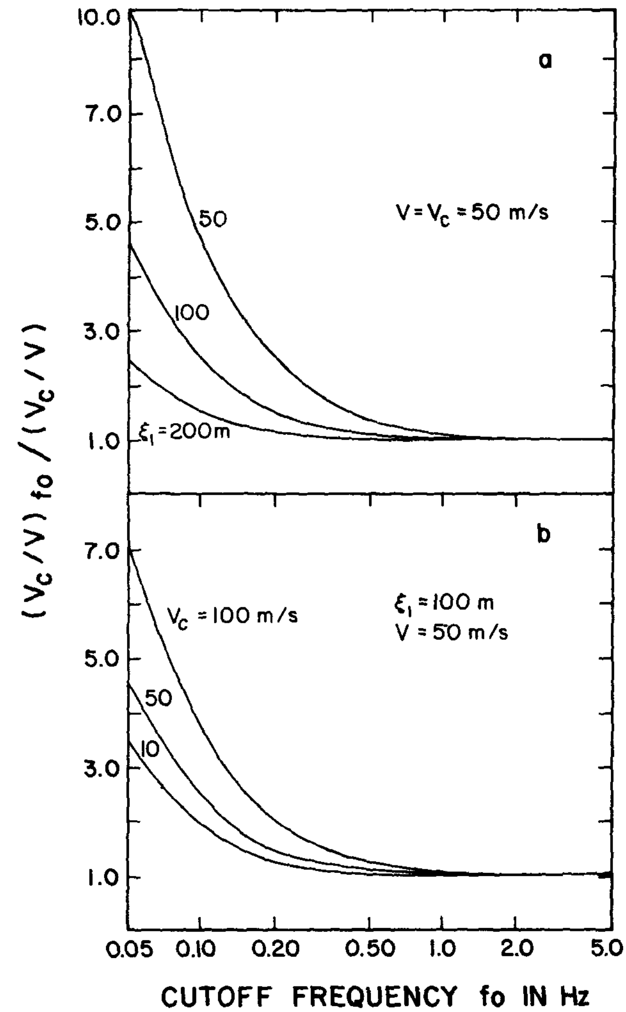

Figure 3. Theoretical variation of the ratio $(V_c/V)_{f_0}$ obtained using a low-pass filter with cut-off frequency f_0 to the ratio V_c/V as a function of f_0 for (**a**) three cases with $\xi_1 = 50$, 100 and 200 m respectively and V, V_c constant at 50 m/s, (**b**) three cases with $V_c = 10$ m/s, 50 m/s and 100 m/s, $\xi_1 = 100$ m and $V = 50$ m/s.

increases as the filtering increases (lower f_0). The increase is larger for smaller scale size. Figure 3b shows similar variations for different values of V_c with $\xi_1 = 100$ m. The ratio shows a larger increase at a higher V_c value.

5. Effect of filtering on scale size

The scale size can be found from (20) and (21)

$$(\xi_s)_{f_0} = \xi_1(1 + V_c^2/\pi^2 f_0^2 \xi_1^2)^{-1/2}$$
$$[-\ln(0{\cdot}5)(1 + (V^2 + V_c^2)/\pi^2 f_0^2 \xi_1^2)]^{1/2}, \quad (37)$$

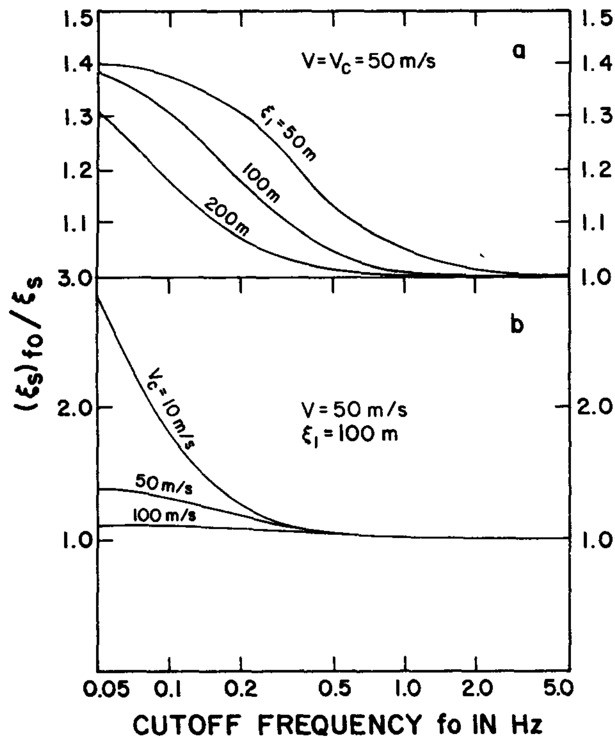

Figure 4. Theoretical variation of the ratio of the scale size $(\xi_s)_{f_0}$ obtained using a low-pass filter with cut-off frequency f_0 to the scale size ξ_s as a function of f_0 for (**a**) three cases with $\xi_1 = 50$ m, 100 m and 200 m and $V = V_c = 50$ m/s, (**b**) for three cases with $V_c = 100$, 50 and 10 m/s respectively and $\xi_1 = 100$ m and $V = 50$ m/s.

which shows an increase in the scale size with filtering. The relative increase is given by the relation

$$(\xi_s)_{f_0}/\xi_s = (1 + V_c^2/\pi^2 f_0^2 \xi_1^2)^{-1/2}$$

$$[1 + (V^2 + V_c^2)/\pi^2 f_0^2 \xi_1^2]^{1/2}, \tag{38}$$

$$= 1 \text{ as } f_0 \to \infty$$

$$= [(V^2 + V_c^2)/V_c^2]^{1/2} \text{ as } f_0 \to 0, \tag{39}$$

which is the maximum limit of the increase. The variation of $(\xi_s)_{f_0}/\xi_s$ as a function of f_0 is shown in figure 4a for cases when $V = V_c = 50$ m/s and for different scale sizes of 50 m, 100 m and 200 m/s. For $f_0 = 1$ Hz and beyond (100 m scale size) there is no significant effect of filtering; however with increasing filtering there is an increase in this ratio. The smaller the scale size the greater the effect. As given by (39) the maximum increase in scale size would be $(2)^{1/2}$ for $V = V_c$. This is evident by the curve for $\xi_1 = 50$ m. In figure 4b the relative increase in scale size is shown for different values of V_c. Here $\xi_1 = 100$ m and V is 50 m/s. The change is marginal for $V_c = 100$ m/s, significant for $V_c = 50$ m/s and very large (nearly a factor of 3) for $V_c = 10$ m/s. This is in accordance with (39).

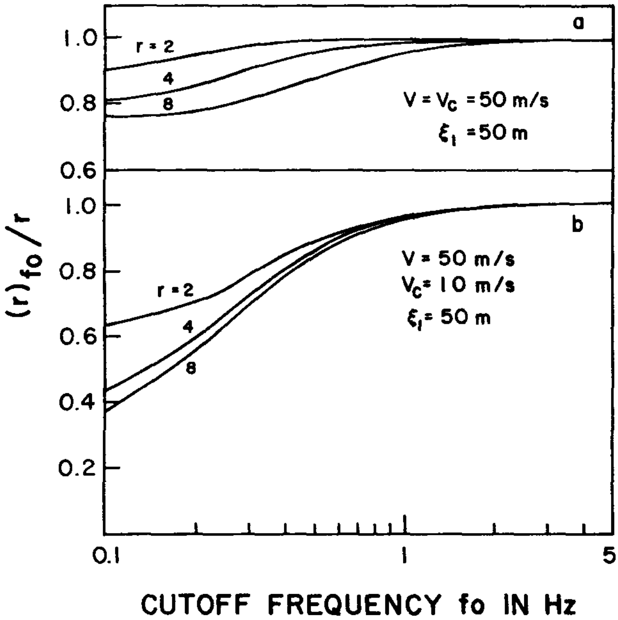

Figure 5. Theoretical variation of the ratio of the axial ratio $(r)_{f_0}$ obtained using a low-pass filter of cut-of frequency f_0 to the axial ratio r for (**a**) three cases with $V = V_c = 50$ m/s, semi-minor axis $\xi_1 = 50$ m and axial ratios of 2, 4 and 8, (**b**) three cases with $V = 50$ m/s, $V_c = 10$ m/s, $\xi_1 = 50$ m and axial ratios of 2, 4 and 8.

To investigate the effect of filtering on the axial ratio (r) of the characteristic ellipse, representing average scale size it must be noted that if the irregularities are isotropic the effect of filtering along different directions will be equal and hence no effect will be observed on axial ratio. For anisotropic irregularities, like those observed at magnetic equatorial latitudes, there would be different quantities of filtering effect observed in the scale sizes due to the vast differences in scale size along the N–S and E–W axes. Since the scale size along E–W axes is smaller, filtering would increase the scale size more along the E–W axes resulting in an apparent reduction in the axial ratio.

The reduction in the axial ratio has been computed from (38) and shown in figure 5. Here the scale size of 50 m has been chosen along the minor axis and 100 m, 200 m and 400 m along the major axis to give axial ratio values of 2, 4 and 8. In figure 5a are shown the values of $(r)_{f_0}/r$ as a function of f_0 for a case $V = V_c = 50$ m/s. There is no change in $(r)_{f_0}/r$ for f_0 values above 1 Hz. For lower values there is a decrease. The reduction is smaller for $r = 2$ (0·9 at 0·1 Hz) and enhanced for $r = 8$ (0·77 at 0·1 Hz). Similar set of curves for another case with $V = 50$ m/s and $V_c = 10$ m/s are shown in figure 5b. In this case the reduction is considerable with $(r)_{f_0}/r$ values of 0·56 (at 0·1 Hz) and 0·31 for $r = 2$ and 8 respectively.

6. Experimental observations

A number of spaced fading records obtained earlier at Tiruchirapalli have been analysed to examine the effect of low-pass filtering. Running mean type of filters with

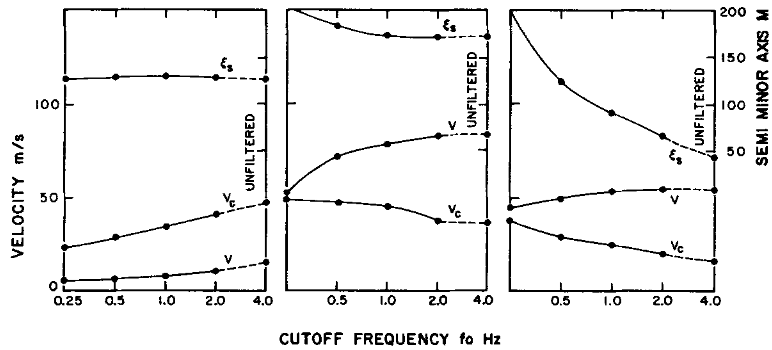

Figure 6. Variation of the true drift velocity V, characteristic velocity V_c and the scale size ξ_s with the cut-off frequency of the low-pass filter f_0 obtained from experimental observations conducted earlier at Tiruchirapalli.

cut-off frequencies varied in steps from 0·125 Hz to 2 Hz (filter widths varying from 0·5 to 10 s) were used in the analysis. A few samples of the results are shown in figure 6, where the variation of V and V_c, V_c/V and the E–W scale size ξ_s are plotted as a function of the cut-off frequency of the filter. In figure 6a is shown a case where the true drift velocity V is only 13 m/s and the characteristic V_c is 45 m/s. The unfiltered values are marked in the figure and joined by dashed lines to the filtered values. Since the sampling process also acts as a filter the unfiltered values are plotted at a filter cut-off frequency of 4 Hz corresponding to the sampling interval of 0·25 s used in digitizing the data. With filtering, V decreases to 4 m/s and V_c decreases to 21 m/s. Thus V_c/V increases from 3·46 to 5·25. These results are expected, as shown on theoretical grounds. There is hardly any variation in ξ_s. This is also in agreement with the findings as the limiting value of an increase in scale size is given by $[(V^2 + V_c^2)/V^2]^{1/2}$ and for $V_c \gg V$ there would be hardly any change in ξ_s with filtering. An example with $V > V_c$ is shown in figure 6b. The unfiltered values are 83 m/s and 37 m/s for V and V_c respectively. V decreases to 53 m/s whereas the value of V_c increases to 49 m/s. Thus while V decreases, V_c increases. The ratio V_c/V also increases from 0·45 to 0·92. These results are in agreement with the theoretical results which show an increase in V_c when $V^2/\pi^2 f_0^2 \xi_1^2 \gg 1$. The scale size ξ_s increases from 171 m to 203 m. Finally in figure 6c is shown an example where V is much larger than V_c. Here the unfiltered values are 55 m/s for V and 16 m/s for V_c. The true drift velocity V decreases to 45 m/s while V_c increases to 38 m/s. The ratio V_c/V increases from 0·29 to 0·84. The scale size shows a large increase in this case from 46 m to 202 m. These results are in conformity with those derived on theoretical grounds.

To allow a proper comparison of the filter effects on experimental records with the theoretical findings, the results of figure 6 are plotted in a different form in figure 7. Here the ratios V_{f_0}/V, $(V_c)_{f_0}/V_c$, $(V_c/V)_{f_0}/(V_c/V)$ and $(\xi_s)_{f_0}/\xi_s$ are plotted as functions of f_0 for the three examples. In figure 7a is the case when $V_c \gg V$. The ratios V_{f_0}/V and $(V_c)_{f_0}/V_c$ decreases with filtering while $(V_c/V)_{f_0}/(V_c/V)$ increases with filtering. $(\xi_s)_{f_0}/\xi_s$ remains independent of filtering. These are in accordance with the theoretical results for the condition $V_c \gg V$. In figure 7b is the case when $V > V_c$. Here V_{f_0}/V decreases while $(V_c)_{f_0}/V_c$, $(V_c/V)_{f_0}/(V_c/V)$ and $(\xi_s)_{f_0}/\xi_s$ increase with filtering. Finally in figure 7c is a case when $V \gg V_c$. Here again V_{f_0}/V decreases while $(V_c)_{f_0}/V_c$, $(V_c/V)_{f_0}/(V_c/V)$ and $(\xi_s)_{f_0}/\xi_s$ increase with filtering. However, the increase in

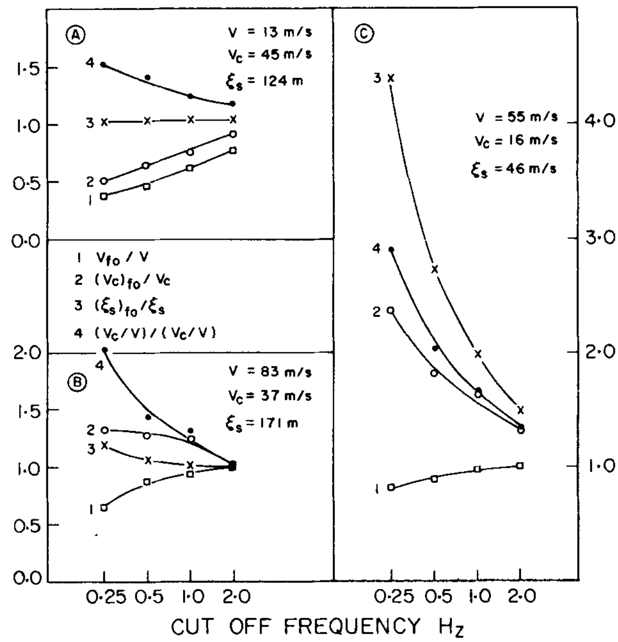

Figure 7. Variation of the ratio V_{f_0}/V, $(V_c)_{f_0}/V_c$, $(V_c/V)_{f_0}/(V_c/V)$ and $(\xi_s)_{f_0}/\xi_s$ with cut-off frequency f_0 of the low-pass filter obtained from the experimental observations shown in figure 6.

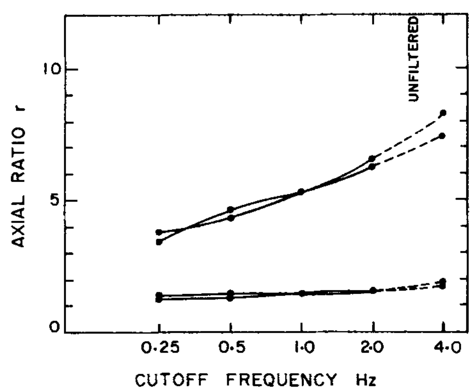

Figure 8. Variation of the axial ratio r, of the ground patterns with the cut-off frequency of the low-pass filter f_0 obtained from experimental observations conducted earlier at Tiruchirapalli.

the last three parameters in this case is larger than the example in figure 7b. As shown earlier the ratio $(V_c)_{f_0}/V_c$ and $(\xi_s)_{f_0}/\xi_s$ will show large increases due to filtering when $V \gg V_c$. However the ratio $(V_c/V)_{f_0}/(V_c/V)$ shows a larger increase when V_c is large, or when the scale size is small. In the example 7c the scale size is only 46 m as compared to 124 m in the example of 7a. Due to this reason $(V_c/V)_{f_0}/(V_c/V)$ increases more in 7c than in 7a. The variations with filtering in all the parameters shown in figure 6 are therefore in conformity with the theoretical results discussed earlier.

The effect of filtering on the axial ratio r of the ground pattern is shown in figure 8.

Here two cases each have been chosen for near isotropic patterns ($r \approx 2$) and anisotropic ($r \approx 8$) patterns. When patterns are near-isotropic filtering hardly affects the axial ratio but for anisotropic cases the axial ratio decreases, and in the examples shown here it decreases from half its value *i.e.* about 8 to about 4. These results are also in conformity with the theoretical findings.

7. Conclusion

It has been shown theoretically that the effect of low-pass filtering-spaced receiver records before subjecting them to full correlation analysis will decrease the V_c' and V, and increase V_c/V and the scale size. V_c decreass unless $V \gg V_c$ when it increases.

The effect of low-pass filtering is noted only when $f_0 \ll V_c/\xi_1$. The quantity ξ_1/V_c has been regarded as the life-time of the irregularity. Thus the effects of a low-pass filter on various parameters are noted only when fading components with periods of the order of the life-time are removed by the filtering. As V_c approaches zero the life-time tends to infinity *i.e.* the irregularity does not change. Hence when the fading patterns can be assumed to be frozen the filter does not affect any parameter obtained by full correlation analysis. It is only when V_c is large that filtering beyond certain limits could alter the derived results. For ionospheric drift applications with typical values of the scale size of 100–200 m and $V = V_c = 50$ m/s, the limiting value of f_0 comes out to be around 1/2 Hz to 1 Hz.

Experimental observations at the equatorial station of Tiruchirapalli have been subjected to low-pass filters with different cut-off frequencies, and the effect of filtering on different parameters studied. It is shown that the experimental observations support the theoretical findings.

Acknowledgement

Sincere thanks are due to Dr B H Briggs for critically going through the manuscript and suggestions.

References

Briggs B H, Phillips G J and Shinn D H 1950 *Proc. Phys. Soc.* **B63** 106
Briggs B H 1968 *J. Atmos. Terr. Phys.* **30** 1777
Chandra H and Briggs B H 1978 *J. Atmos. Terr. Phys.* **40** 541
Fooks G F 1965 *J. Atmosp. Terr. Phys.* **27** 979
Sprenger K and Schminder R 1969 *J. Atmos. Terr. Phys.* **31** 1085